JOURNAL OF FORENSIC SCIENCES

J Forensic Sci, 2017
doi: 10.1111/1556-4029.13524
Available online at: onlinelibrary.wiley.com

PAPER

CRIMINALISTICS

Jimmie C. Oxley,[1] *Ph.D.; James L. Smith*,[1] *Ph.D.; Evan T. Bernier*,[2] *Ph.D.; Fredrick Sandstrom*,[3] *M.S.; Gregory G. Weiss*,[3] *M.S.; Gunther W. Recht*,[3] *B.A.; and David Schatzer*,[4] *B.S.*

Characterizing the Performance of Pipe Bombs*

ABSTRACT: Pipe bombs of steel or PVC fragment in reproducible patterns when similarly configured. The power of the explosion correlates with number, mass, and size of the fragments recovered, where a large number of small, low-mass fragments indicate a high-power event and vice versa. In discussing performance, describing pipe fragmentation pattern by fragment weight distribution mapping (FWDM) or fragment surface area distribution mapping (FSADM) was useful. When fillers detonated, detonation velocities of ~4.4 mm/μs were measured. In such cases, side walls of the pipe were thrown first; the average fragment velocity was ~1000 km/s. In deflagrations, the end cap was first thrown; fragment velocities were only ~240 km/s. Blast overpressures varied; at 10 feet, 2 × 12 inch steel pipes containing ~550 g of detonable mixture produced overpressures of 5–6 psi; similar nondetonating pipes produced less than 2 psi. Maximum fragment throw distances were 250–300 m, with an average of ~100 m.

KEYWORDS: forensic science, pipe bombs, fragmentation, Gurney energies, fragment weight distribution maps, detonation velocity, fragment velocity, safe radius

Pipe bombs are the most common and pervasive improvised explosive devices (IEDs) encountered by law enforcement personnel in USA. A Bureau of Alcohol, Tobacco Firearms and Explosives (ATF) report found that between 1993 and 1997, 34% of the 10,000 bombings or attempted bombings recorded involved pipe bombs. The "explosive" fillers consisted of flammable liquids (30%), black powder (10%), smokeless powder (8%), photo and fireworks powders (17%), match heads (2%), and unspecified chemicals (26%) (1). Figures for 2015 for explosions showed little change in black powder and black powder substitutes (9%) and smokeless powder (4%) maintains their place, while fireworks and flash powders appear to be more popular (46%) with pipes remaining a popular container.

Law enforcement and other emergency response personnel who must respond to bombing incidents are faced with several issues. In cases where the device has not functioned, the immediate issue is to cordon off a safe distance to which the scene must be evacuated of bystanders and nonessential personnel. Knowledge of the potential threat for human injury and property damage is necessary for the bomb squad to safely apply render safe procedures on the unexploded device. In cases where the device has already functioned, crime scene investigators and evidence recovery teams must locate, identify, and collect as much physical evidence as possible to support subsequent forensic analyses. In the case of a pipe bomb, this physical evidence includes, but is not limited to, pipe and end-cap fragments, unburned powder residue, and initiator components. The parameters used to cordon off a safe distance for an intact device can also be used to determine an evidence recovery zone or envelope for a device that has functioned.

The possible variations in pipe bomb configurations are enormous. This alone makes any kind of systematic characterization and quantification of their effects and postblast fragmentation challenging. However, previous research by members of this group definitively showed that the fragmentation characteristics of pipe bombs are both reproducible and quantifiable and can be related to their original construction (2). The research presented here has been conducted to further verify and validate those original findings, as well as to generate additional experimental data on the postblast signatures and potential effects of pipe bombs. Four test series were performed; with a total of 94 pipe bombs test fired. The goal of test series A was the complete recovery and analysis of pipe bomb fragments along with a limited collection of filler burn rate or detonation rate measurements. Test series B involved the measurement of pipe bomb fragment velocities. Test series C measured blast overpressure and impulse as a function of distance and direction from the pipe bomb, and in test series D, the distance metal pipe fragments were thrown in a flat, open area was determined. All four test series yielded a multitude of information about the mass, morphology, and distribution of collected pipe fragments. Overpressure/impulse, fragment velocity, and throw distance values were ultimately used to define the realistic hazards associated with pipe bombs.

[1]Chemistry Department, University of Rhode Island, 140 Flagg Road, Kingston, RI.
[2]Vantage Resourcing Solutions, 19 Mason Street, Beverly, MA.
[3]Applied Research Associates, 7921 Shaffer Pkwy, Littleton, CO.
[4]David Schatzer, Washington, DC.
*Funding provided by Technical Support Working Group/Combating Terrorism Technical Support Office.

Received 9 Nov. 2016; and in revised form 13 Feb. 2017; accepted 8 Mar. 2017.

Experimental Section

Pipe Materials and Sizes

Configurations of the pipe bomb devices studied included three materials: domestically produced ASTM A53 galvanized steel with a continuous butt-welded (CBW) seam; foreign produced ASTM A53 galvanized steel with an electric resistance-welded (ERW) seam; and domestically produced ASTM D175 polyvinyl chloride (PVC). All steel pipes were threaded at both ends and closed with threaded, galvanized cast iron end caps. Domestically produced steel pipes were capped with domestically produced, flat-topped end caps, and the foreign produced steel pipes were capped with foreign produced dome-topped end caps. The PVC pipes were closed at each end with PVC end caps attached with PVC cement.

The pipe sizes (and designations for the purpose of this effort) that were tested consisted of 1 in. pipe size × 6 in. length (1 × 6, or "1 inch") and 2 in. pipe size × 12 in. length (2 × 12 or "2 inch"). All 1-inch pipes tested were ASTM schedule 40, which specifies a nominal outside diameter (OD) of 1.315 inch and a nominal wall thickness of 0.133 inch for both steel and PVC pipe. The 2-inch pipes tested were also ASTM schedule 40, which denotes a nominal outside diameter (OD) of 2.375 inches, and a nominal wall thickness of 0.154 inch for both steel and PVC pipe.

Pipe Fillers

The baseline energetic pipe bomb fillers were black powder (FFFg) and various smokeless powders including Alliant Bullseye and Alliant Herco. Analysis of the fragmentation patterns from the first 10 pipes tested indicated that the Herco was similar in performance to Bullseye and was substituted with the slower burning Alliant Reloder 22 smokeless powder. To correlate the results of this study with the previous pipe bomb study (2), selected pipe bombs were also tested with Alliant Red Dot, Alliant 2400, and IMR-4227 smokeless powder fills. The Alliant powders were all double base, containing both nitroglycerin (NG) and nitrocellulose (NC). Table 1 includes nitroglycerin (NG) content, grain shape, and relative quickness or burn rate. IMR-4227, the only non-Alliant smokeless powder included in this study, was a single-base powder, containing only NC. Its "relative quickness" has been reported to be somewhat slower than Alliant 2400 based on unverified information from the Internet. Initially, C-4 was selected as a reference high explosive, but fragmentation of a 1″ × 6″ CBW steel pipe was far too extensive. Subsequent reference shots were assembled using flaked TNT which had performance close to that of smokeless powders. After one end cap was sealed on the pipe, most pipes were filled with powder to within 0.06 inches from the end of the threading. Seven partially filled pipe bombs (1/2, 2/3, and ¾) were assembled for a series of horizontal shots in test series A.

TABLE 1—*Description of smokeless powders.*

Powder	Relative Quickness	% NG	Grain Shape
Bullseye	Fast	40	Flake
Red Dot	Fast	20	Flake
Herco	Medium	20	Flake
2400	Med. slow	15	Flake
Reloder 22	Slow	11	Single perf

Initiators

The baseline pipe bomb configuration included an initiator mounted through a 1/8″ diameter hole in one end cap. Those pipes oriented vertically in test series A were initiated through the top end cap. A few steel pipe bombs were initiated by an electric match mounted through a 1/8″ diameter hole in the center of the pipe wall opposite the seam. The baseline initiator was an electric match [Flash Match (F Head)–Luna Tech, Inc], containing 0.05 g of pyrotechnic composition. The match was ignited with a fireset, custom built by Applied Research Associates, Inc. To determine the maximum power of the pipe bombs, an exploding bridgewire (EBW) detonator was also used in pipes filled with smokeless powder or high explosives (C-4, TNT). The EBW was a RISI RP-81, containing 450 g of RDX with an output equivalent to a #8 blasting cap. It was initiated using a CDUC44 fireset, manufactured by Components, Inc. Two steel 2″ × 12″ pipes were initiated using a 6 inch length of hobby fuse to compare their performance to pipes initiated with an electric match.

Series A—Fragment Recovery

Pipe bombs were initiated both vertically and horizontally in fixtures constructed from galvanized steel culverts (Fig. 1). The vertical fixture was lined with eight radial recovery packs. Only four packs were required in the horizontal fixture as it was half buried on its side. Each recovery pack was composed of sixteen ½″ acoustic ceiling tiles cut to a 48″ height × 24″ width. The panel widths within a pack were tapered to the inside of the culvert to accommodate the cylindrical geometry. Each pack was backed with three ½″ Celotex panels and ¾″ plywood, and fronted with an aluminum witness panel. Packs were secured to the fixture with a length (48″) of steel hat channel that was attached to both the left and right edges of all the plywood backings. Two 48″ × 48″ recovery packs were positioned at the top and at the bottom (vertical fixture) or side (horizontal) openings of the culvert. A small stand-off between the ends of the culvert and these recovery packs provided blast venting. All recovery packs were labeled and marked with respect to their position and orientation in the test fixture. The radial packs in the vertical test fixture were labeled as AB, BC, CD, DE, EF, GH, and HA depending on the two alphabetically designated posts which the pack was positioned between. The top and bottom recovery packs in the vertical fixture were labeled as such, and their orientation relative to the radial packs was marked. Radial packs in the horizontal test fixture were labeled only GH, HA, AB, and BC as half of the culvert was buried. The end packs positioned at the sides of the horizontal fixture were also labeled "top" and "bottom." Pipe bombs, which were vertically aligned, were suspended by a wire just under the lip of the upper end cap and centered vertically and horizontally in the recovery fixture. The pipe bombs were positioned so that the pipe seam faced the metal joint designated "A," located between recovery packs AB and HA. In the horizontal fixture, the pipe bombs were placed directly upon paving tiles laid on the ground and were aligned with the center of the recovery packs. The bombs were shot with the seam either straight up or straight down. In either case, the strip of pipe, which sat on the paving tiles, was flattened, and bits of paving tile were often found in the pipe threads. Immediately following each shot, pipe fragments on the ground were collected and the recovery packs were removed to a work area where fragments could be located and removed with magnets and screw drivers as needed.

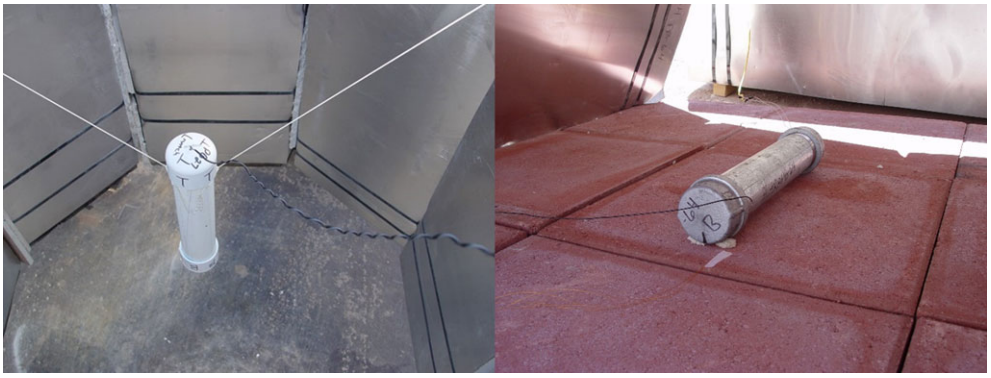

FIG. 1—*Pipes were oriented for initiation both vertically (left) and horizontally (right).*

Velocity of Detonation (VOD) (Series A)

VOD measurements were recorded in conjunction with some of the fragment recovery tests. It was necessary to utilize detectors, which would not affect the pipe fragmentation. Thus, piezoelectric pins or fiber optic probes mounted in holes drilled within the pipe wall could not be used. Rather, lengths of small diameter (32 gauge −0.008″) polyester-insulated copper magnet wire were positioned at discrete intervals along the length of the pipe surface and used as electrical "make" switches. A small loop was made at the end of each wire and taped to the pipe with the leading edge of the loop located at premeasured marks along the length of the pipe. A voltage was applied to each wire, while the pipe was electrically grounded. For steel pipes, the pipe was wired directly to the time-of-arrival circuitry. For PVC pipes, a strip of copper tape affixed to the length of the pipe served as the electrical ground, and the make wires were fastened to the tape. When the pipe ruptured, the shock wave associated with the detonation front propagated through the pipe walls and crushed the insulation on the magnet wire, resulting in electrical contact between the wire and the grounded pipe wall. Associated electrical circuitry registered each switch closure and generated a single pulse that was recorded on a digital storage oscilloscope.

Fragment Velocity (Series B)

The arena for fragment velocity testing consisted of a pipe bomb balanced on the end of a vertically positioned cardboard tube, four flash panels, and two high-speed digital cameras as illustrated in Fig. 2. Each pipe bomb was placed horizontally on top of the notched cardboard tube, 36″ above ground level. The cardboard tube was slipped over a steel pipe welded to a steel base plate which was partially filled with sand to prevent

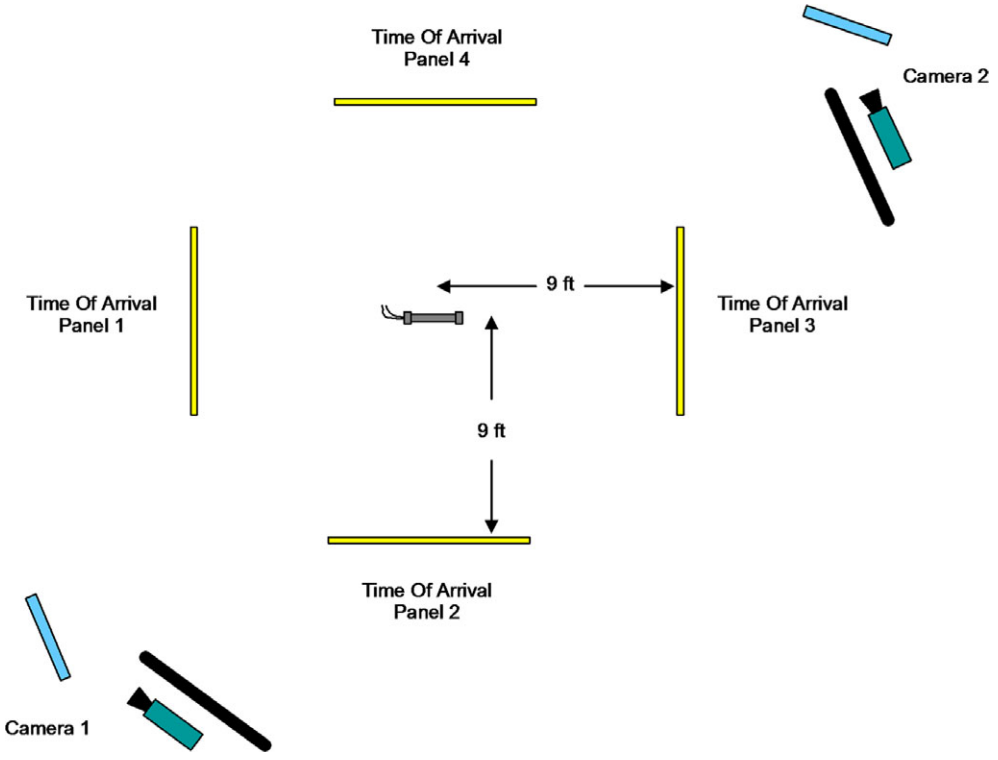

FIG. 2—*Fragment velocity testing arena (not to scale).*

fragment damage to the stand. The four flash panels were located ~9 ft. from the pipe bomb center. The two flash panels positioned toward the ends of the pipe (panels 1 and 3) were used to measure the arrival time of the end-cap fragments, while panels 2 and 4 were used to measure the arrival time of pipe wall fragments. Each flash panel was made from 48″ × 48″ corrugated cardboard attached to a wooden frame. The wooden frame held the center of the flash panels 36 inches above the ground, the same height as the pipe bomb. To provide electrically conductive surfaces, the front surface of each flash panel (the side facing the pipe) was coated with flame-sprayed aluminum, and the back surface was covered with 0.003″ aluminum foil. A differential voltage of 13 VDC was applied between the front and rear surfaces through a "pull-up" resistor. As fragments passed through the flash panel, they shorted the front and rear surfaces of the flash panel, and the output signal dropped to zero. The voltage difference between the front and rear panels was recorded digitally to measure the arrival time of the fragments. The sprayed aluminum on the front of the panels provided a brittle surface that adhered to the cardboard. As the fragments passed through the flash panel, the sprayed aluminum broke cleanly, allowing the voltage between the front and rear panel to pull up repeatedly. This approach allowed the arrival of many fragments to be recorded on each panel. Voltage differences were recorded by a digital data acquisition system and later compared with the initiation time to compute the speed at which each fragment penetrated the panels located ~9 feet away. Two Phantom 7.1 high-speed digital cameras (4600 frames/second) provided an additional measurement of the time of pipe rupture and the time when fragments passed through the flash panels. The flash panel data acquisition and the high-speed digital cameras were triggered simultaneously with the fireset. This configuration permitted simultaneous comparison between the flash panel data and camera images. The trigger signal to the low-voltage fireset passed through a mechanical relay before firing, which resulted in a 6- to 8-ms delay between the trigger point and the "time of first light" observed by the cameras. Pipe bombs initiated by an electric match showed a delay of about 17 ms between the trigger and the break wire. This signal was also recorded by the data acquisition system and provided a start time for each fragment's travel time.

Blast Overpressure (Series C)

For this test series, a number of flaked TNT charges were prepared in cardboard tubes and initiated with detonators to simulate uncased charges. In Table 7, these are labeled Ref. (1) through Ref. (9). All other pipe bombs in this test were prepared as described above. The arena for air blast testing consisted of the pipe bomb, four air pressure gauges on four radial lines to measure the air blast nominally at 5, 10, 15, and 20 feet, and a high-speed, Phantom 7, camera set at 29,000 frames/s to record the fragmentation of the pipe bomb. Figure 3 illustrates the arena layout and the radial alignment of the pressure gauges used to measure the air blast nominally at 5, 10, 15, and 20 feet around the pipe. The pipe bombs were positioned either vertically or horizontally on the ground or at 52 inches above the ground, the same height as the pressure gauges. When the pipe bomb was oriented vertically, it was suspended between two fragment barriers using nylon string, with the initiator at the top. Tests with the pipe bomb positioned horizontally at 52 inches utilized a cardboard tube to support the device. Prior to each test, the distance from the pipe bomb to each gauge was measured and recorded.

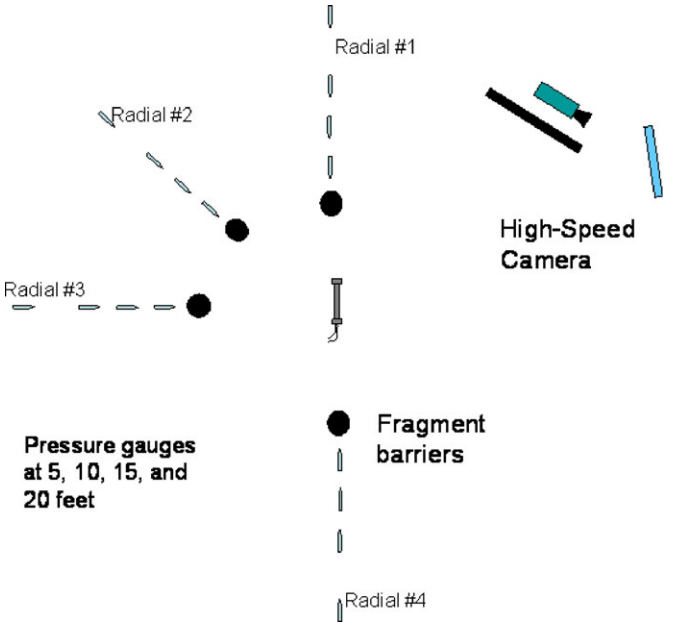

FIG. 3—*Blast overpressure.*

Fragment Throw Distance (Series D)

An illustration of the arena used for fragment throw distance testing can be seen in Figure 4. Each pipe bomb tested was surrounded by 8 pressure gauges aligned in two separate radials with all the gauges 52 inches above the ground and at a nominal distance of 5, 10, 15, and 20 feet from the pipe bomb. A Phantom 7 high-speed digital camera, recording at 4800 frames/second, was used in an attempt to track pipe fragments in flight within the recovery zone.

All the pipe bombs tested were placed at ground level. Initially, they were placed on a steel plate which was replaced with concrete paving stones. The paving stones provided less rebound than the steel plate to the large fragments that were driven down during the explosion. The first test (PB-110) was angled up at 15° to maximize the throw distance of the large, circular end-cap fragment (wafer) that had been observed in fragment recovery and fragment velocity testing. In the remaining tests, each pipe bomb was placed flat.

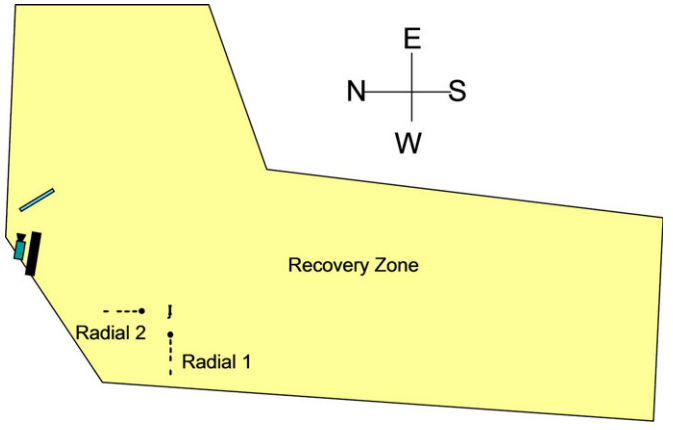

FIG. 4—*Graded recovery area for Fragment Throw Test Series D.*

The end of the pipe bomb opposite the initiator was pointed east (up in Fig. 4) for seven of the nine total tests. For the remaining two tests, the end of the pipe bomb opposite the initiator was pointed south (right in Fig. 4). The primary recovery zone was the larger rectangular portion seen in Fig. 4 extending to the southernmost border of the test zone. The size of this area extended approximately 350 m to the south and 75 m to the east of where the pipe bomb was placed. The ground of this area was composed of freshly graded earth free from large rocks, gravel, and any fragments from previous testing. An additional area to the north and east of the graded earth was also included in the recovery zone. This area was in its natural state, with some trees and large shrubs. It was also searched after each test. Locating fragments in this area was more difficult and presumably less efficient. Areas adjacent to the formal recovery zone were also searched.

The entire recovery zone was searched for fragments after each pipe bomb tested. An attempt was made to use an infrared camera to locate hot fragments. It was ineffective, presumably because the fragments were not large enough to be resolved by the camera that was used. A lineup of people spaced about 10–20 feet apart slowly walked the length of the recovery zone, locating and marking fragments with small flags. Once located, the distance of each fragment from ground zero was measured using a steel tape measure. For fragments further away than 25 feet, a surveying theodolite with laser was used to measure the angle and distance. The fragments were individually tagged at the recovery zone and later characterized by mass and size.

The outside of the pipes used in this test series was painted with high-temperature paint yellow, orange, or blue or left unpainted to identify from which pipe bomb the fragments originated. After each color had been used, a tractor with a large electromagnet was driven over the recovery zone to collect unrecovered fragments.

Pipe Fragment Analysis

All fragments were individually weighted, and their circumference was measured to the nearest tenth of an inch as if each were a perfect rectangle. Using calipers, the thickness of several pieces was determined at several locations, but at some distance from the pipe seam, a region was generally thicker than other areas of the pipe. The extent of thinning of the pip was evaluated in comparison with an unused pipe.

Results and Discussion

Fragment Recovery (Series A)

After each pipe was shot in the recovery fixture, the recovery packs were removed and the inner aluminum witness panels taken for photographic analysis (e.g., Fig. 5). Pipe fragments were extracted from the acoustic tiles by probing perforations in each individual recovery pack with screwdrivers and magnets. Fragments were also collected from the debris on the steel plate underneath the recovery fixture and, with the aid of magnets, from the ground around the fixture. The three-dimensional final location of each recovered fragment was recorded in terms of the following: (i) recovery pack designation (e.g., HA); (ii) recovery pack panel number (1–21, 1 being that closest to the center of the fixture and 21 designated as the plywood on the outside of the recovery pack); and (iii) x–y coordinates on a given panel [i.e., distances (inches) from the bottom and right side of the each panel). Fragments not embedded in the recovery packs were labeled "free."

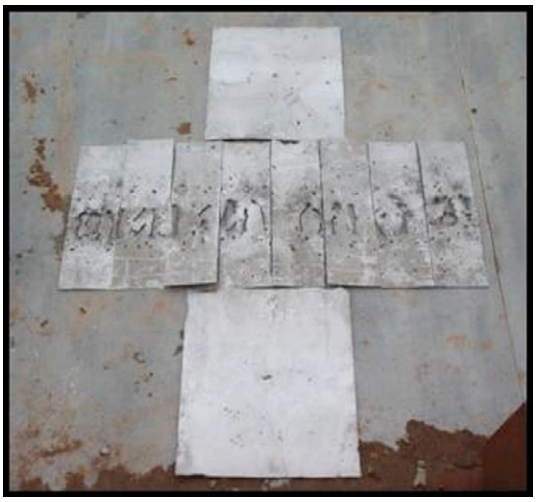

FIG. 5—*Aluminum witness panels from recovery packs.*

Figure 6 is a sample graph of the x-y distribution of pipe and end-cap fragments recovered from a 2″ × 12″ CBW steel pipe filled with Herco smokeless powder and detonated in vertical orientation. Each fragment recovered is represented by a green triangle (pipe) or a purple square (end cap), and the plot represents a view of all eight recovery packs lined up as in Fig. 5. Figure 7 also illustrates this xy positioning of fragments, but each fragment is represented by a sphere with size relative to the mass (g) of the individual fragment. As expected, the majority of the pipe wall fragments were found near the vertical center of the recovery packs and the end caps near the top and bottom of the panels. Fragments generally flew radially outward trending slightly downward due to gravity. A number of the pipe fragments were observed to have aluminum from the witness panels melted onto them.

In addition to the location of each fragment, its mass (g) and aspect ratio (if L × W was at least 2 × 2 cm) were recorded along with a designation as to if it appeared to be metal from the end cap or pipe nipple. This information was recorded for all the collected fragments of each pipe bomb in individual Excel spreadsheets within hours of the shot. Thickness measurements of the larger fragments were made after the fragments were transported to the URI laboratory. Morphological and microstructural changes in the steel were the subject of a separate paper (3).

In fragment recovery test series A, the average percentage of fragments recovered for all pipes was about 87%. In other test series where the pipe fragments were allowed free flight, recovery was significantly lower, an average of ~30%. Table 2 is a summary of data from the 1″ × 6″ steel and the PVC pipe bombs. Table 3 is the summary of the 2″ × 12″ steel pipe bomb data collected. Both tables include two synthesized numerical evaluators for the power of each device (FWDM and FWDMSA), which are described below.

FWDM and FSADM

While visually, the fragmentation of a pipe bomb could be evaluated as reproducible and its relative power estimated, it is useful to use a numerical method to express physical aspects of

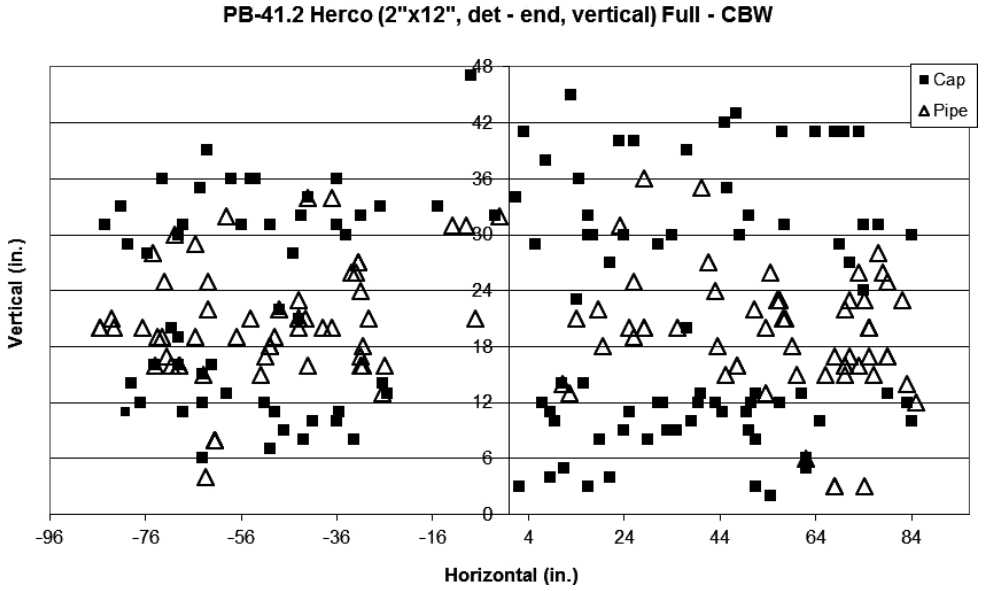

FIG. 6—*XY distribution of fragments from 2" × 12" steel pipe detonated w/Herco filler.*

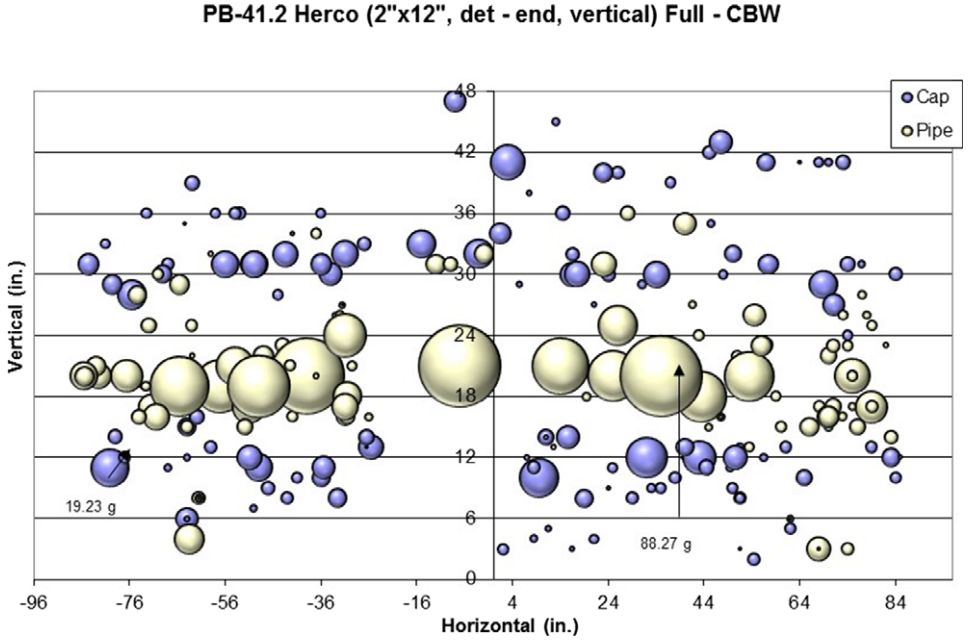

FIG. 7—*XY distribution as in Fig. 6 with bubbles in proportion to fragment mass of data points.*

the fragmentation. Fragment weight distribution map (FWDM) slopes, tentatively identified in the previous study, have proved to be a simple way to characterize the relative power of an exploded pipe bomb (2). The FWDM evaluator compensates for the fact that the total pipe mass or total recovery of the pipe fragments will vary between devices by calculating a percentage of fragment weight directly. The abscissa (x) of the map is the weight of a single fragment (m_x) divided by the total weight of all recovered fragments (M_r) for that pipe (The calculation can be simplified using the weight of all fragments in a given weight category as the numerator. This greatly accelerates the calculation, especially if it is applied to a large number of very small fragments.). The ordinate (y) of the map reflects how much of the pipe is accounted for by the largest pieces. It uses the sum of the single fragment weight (or total weight in the category) with all fragments larger than it [sum ($m_1 + m_2 + m_3 \ldots + m_x$)]. This cumulative weight is divided by the total recovered fragment weight (M_r) for normalization. Furthermore, the logarithm of this value is used, so that the ordinate becomes log {[100 × (fragment weight + all heavier fragment weights)]/(total weight of all fragments)} or

$$\log\left[100\left(\frac{(m_1 + m_2 + m_3 + \ldots m_x)}{M_r}\right)\right] \quad (1)$$

The use of the logarithm tends to minimize minor statistical variations and accentuate major variations. Dividing both the individual fragment weight (x-axis) and the sum of all fragments

TABLE 2—*Pipe bombs steel and PVC (1" diameter steel or 1" or 2" PVC, 100% filled, end cap initiated).*

PB #	Align.	Material	Length (in.)	Type	Fill Mass (g)	Initiator	# Pipe Frags	# Cap Frags	# Total Frags	Mass Total Frag.	% Recovery	Length/ width	FWDM Slope	R^2 value	FWDMSA Slope	R^2 value	Thining (%)
21	Vert.	ERW	6	Black Powder	98	Match	1	7	8	652	97		0.2	0.89			
17	Vert.	CBW	6	Black Powder	98	Match	1	4	5	688	98		0.2	0.87			
58	Vert.	CBW	6	Black Powder	95	DET	1	16	17	684	99		0.7	0.98	1.4	0.98	
56	Vert.	CBW	6	Reloder 22	91	Match	5	5	10	687	98	1.43	1.1	0.64	0.3	0.89	32
39	Vert.	CBW	6	Reloder 22	86	DET	8	28	36	690	99	1.5	1.2	0.88	3.8	0.92	38
72	Horiz	CBW	6	Bullseye	64	DET	12	7	19	39	6		4.3	0.72	4.3	0.72	33
73	Horiz	CBW	6	Bullseye	66	DET	56	37	93	312	45		8.5	0.95	8.5	0.95	45
9	Vert.	CBW	6	Bullseye	66	Match	19	57	80	673	97	2.05	1.9	0.82	0.8	0.81	67
13	Vert.	ERW	6	Bullseye	64	Match	79	62	144	615	93	2.5	12.2	0.96	7.9	0.98	36
34	Vert.	CBW	6	Bullseye	64	DET	116	113	276	620	89	2.86	49.6	0.96	33.7	0.96	37
2	Vert.	CBW	6	Herco	60	Match	20	42	65	656	92	2.26	2.1	0.85	2.6	0.64	67
1	Vert.	CBW	6	Herco	59	Match	23	49	72	632	91	2.69	2.2	0.86	1.7	0.96	65
38	Vert.	CBW	6	Herco	59	DET	92	80	>196	605	86	3.56	28.0	0.97	9.7	0.96	38
31	Vert.	CBW	6	C4	137	DET	230	140	>747	354	51	3.74	71.0	0.93	28.2	0.95	41
T1	Vert.	CBW	6	TNT	82	DET	67	49	116	408	58	2.8	25.0	0.98	12.2	0.98	24
57	Vert.	CBW	6	TNT	79	DET	76	73	149	542	77	2.85	27.6	0.98	10.9	0.96	31
27	Vert.	PVC	12	Reloder 22	655	Match	435	31	466	431	93	3.00	10.7	0.93	12.6	0.94	
28	Vert.	PVC	12	Reloder 22	665	DET	108	42	858	404	87	3.26	12.6	0.91	7.4	0.89	
26	Vert.	PVC	12	Reloder 22	655	DET	145	51	671	388	83	3.12	17.0	0.83	4.0	0.96	
25	Vert.	PVC	12	Black Powder	714	Match	75	15	192	435	93	2.69	7.8	0.94	5.5	0.89	
30	Vert.	PVC	12	Bullseye	467	Match	17	13	64	466	100	3.04	8.3	0.96	9.3	0.95	
60	Vert.	PVC	6	Bullseye	59	DET	n/a	n/a	>318	36	28	3.23	53.5	0.88	3.4	0.93	
29	Vert.	PVC	12	Bullseye	460	DET	3	n/a	194	36	8		39.1	0.93	0.4	1.00	
33	Vert.	PVC	12	TNT	599	DET	20	3	239	55	12	4.44	38.8	0.97	8.2	0.96	

TABLE 3—*2″ × 12″ steel pipe bombs (averages for test series A& B only) (C, center initiated).*

PB #	Align.	Material	Filler	Mass Fill (g)	Initiator	Number Frags Pipe	Cap	Total	Total Frag (g)	Avg Depth # tiles pipe	cap	% Recovery	frag L/w	FWDM Slope	R^2	FWDMSA Slope	R^2	% Thin
7	Vert.	ERW	Reloder 22	578	Match	10	6	16	2221	5.0	6.5	97	3.1	1.6	0.97	1.0	0.75	77
59	Vert.	CBW	Reloder 22	717	Match	10	4	14	2485	6.6	1.0	97	2.0	1.9	0.80	1.2	0.80	64
62	Vert.	CBW	Reloder 22	696	Match	3	3	6	2595	12.7	2.7	100	3.5	2.5	0.71	2.1	0.98	71
41	Vert.	CBW	Reloder 22	685	DET	23	32	55	2624	7.1	3.6	99	3.4	3.0	0.93	2.4	0.91	67
79	Hor.	CBW	Reloder 22	687	DET	47	24	71	1204			47		1.4	0.87	1.4	0.87	64
78	Hor.	CBW	Reloder 22	696	DET	15	10	25	1232			47		1.1	0.88	1.1	0.88	79
107	Hor.	CBW – US	Reloder 22	703	DET	4	9	13	767			41	2.8	1.9	0.94			70
109	Hor.	ERW	Reloder 22	708	Match	4	8	12	1503			34	2.2	0.7	0.80			74
108	Hor.	CBW – US	Reloder 22	753	Match	10	24	34	1120			55	2.2	0.8	0.71			66
Avg Reloader 22 @ match-frag wt 203g						**8**	**4**	**12**		**8.1**	**4.0**	**98**	**2.9**	**2.0**		**1.4**		
10	Vert.	CBW	Bullseye	459	Match	104	104	352	2333	13.1	11.4	87	3	8.0	0.71	2.9	0.71	59
55	Hor.	CBW	Bullseye	481	Match	373	104	477	2099	11.2	9.2	80	2.8	9.5	0.86	9.6	0.90	56
54	Hor.	CBW	Bullseye	491	Match	300	119	419	1989	12.2	9.6	79	3.4	9.7	0.83	7.2	0.86	47
15	Vert.	ERW	Bullseye	472	Match	>193	111	>307	2010	12.8	9.6	88	2.6	13	0.84	8.9	0.77	65
46	Vert.	CBW	Bullseye	490	match C	180	371	551	2170	10.2	11.9	83	2.8	14	0.79	7.3	0.99	49
12	Vert.	CBW	Bullseye	463	Match	>288	142	433	2286	12.3	11.4	86	3	16	0.83	12	0.88	49
61	Vert.	CBW	Bullseye	503	Match C	>65	135	>200	2261	8.0	12.4	90	2.6	20	0.96	1.9	0.81	64
70	Vert.	CBW	Bullseye	463	Hobby	200	141	341	2122	12.0	11.7	81	2.7	22	0.92	4.9	0.80	61
90	Hor.	CBW – US	Bullseye	492	Match	29	45	77	663			24	3	1.5	0.51			46
Avg Bullseye @ match-frag wt 6.7g						**198**	**141**	**339**		**11**	**10.9**	**84**	**2.9**	**14**		**6.9**		
36	Vert.	CBW	Bullseye	474	DET	318	218	647	2218	11.1	10.9	84	5.2	34	0.86	22	0.89	60
37	Vert.	CBW	Bullseye	481	DET	365	247	621	2235	9.8	10.3	86	4.4	39	0.94	26	0.95	41
69	Hor.	CBW	Bullseye	463	DET	365	208	573	2210	11.5	8.4	84	5.1	40	0.9	3.8	0.79	41
64	Hor.	CBW	Bullseye	485	DET	470	238	708	2174	13.3	12.1	82	4.1	73	0.99	9.4	0.57	43
68	Vert.	ERW	Bullseye	483	DET	418	195	614	1892	11.9	11.8	84	4.3	88	0.94	46	0.96	48
74	Hor.	CBW	Bullseye	481	DET	42	19	61	177			7		12	0.96	12	0.96	52
75	Hor.	CBW	Bullseye	485	DET	78	30	108	383			15		8.6	0.92	8.6	0.92	57
89	Hor.	CBW – US	Bullseye	481	DET	32	125	157	627			23	3	2.3	0.47			41
Avg Bullseye @ detonator frag wt 3.4g						**387**	**221**	**608**		**11.5**	**10.7**	**84**	**4.6**	**55**		**21**		
63	Hor.	CBW	Bullseye	247	DET	174	168	347	2326	10.2	9.5	89	3.1	16	0.92	7.6	0.97	48
49	Hor.	CBW	Bullseye	247	Match	34	20	54	2283	9.1	7.6	87	3.8	2.8	0.92	2.0	0.91	55
48	Hor.	CBW	Bullseye	238	Match	21	19	40	2263	11.5	7.2	88	3.8	4.6	0.98	2.9	0.95	54
51	Hor.	CBW	Bullseye	299	Match	29	112	141	2495	8.0	9.5	94	2.8	2.7	0.88	2.7	0.93	60
50	Hor.	CBW	Bullseye	304	Match	28	31	59	2509	8.4	10.0	95	3.5	4.7	0.99	2.2	0.93	69
52	Hor.	CBW	Bullseye	365	Match	114	95	209	2264	11.0	9.4	89	3.1	3.7	0.85	3.1	0.74	44
53	Hor.	CBW	Bullseye	367	Match	90	103	193	2295	11.6	8.2	87	3.1	9.4	1	4.6	0.94	48
Avg Bullseye (horz) @ match frag wt 16g						**53**	**63**	**116**		**10**	**8.7**	**90**	**3.4**	**4.6**		**3**		
3	Vert.	CBW	Herco	425	Match	60	142	214	2450	11.2	12	93	3	3.2	0.81	1.2	0.82	38
4	Vert.	CBW	Herco	429	Match	106	145	273	2497	11.7	11	94	3	5.1	0.8	2.8	0.87	64
41-2	Vert.	CBW	Herco	431	DET	177	197	427	2319	9.8	8.9	89	5.4	32	0.97	19	0.99	59
40	Vert.	CBW	Herco	432	DET	217	187	455	2311	10.7	9.4	89	5.7	34	0.97	21	0.94	56
65	Vert.	CBW	IMR 4227	651	DET	313	185	499	2288	10.6	9.8	88	3.1	29	0.89	26	0.91	54
76	FV	CBW	IMR 4227	642	DET	70	21	91	637			24		6.2	0.92	6.2	0.92	52
77	FV	CBW	IMR 4227	678	DET	23	10	33	445			18		3.9	0.95	3.9	0.95	49
98	Hor.	CBW – US	IMR 4227	652	DET	53	95	148	1171			43	3.3	4.1	0.57			53
99	Hor.	CBW – US	IMR 4227	645	Match	7	33	40	1642			60	2.2	0.8	0.83			68
23	Vert.	ERW	Black Powder	753	Match	6	6	12	2214	5.2	6.5	95	2.5	1.7	0.92	0.6	0.98	84
47	Vert.	CBW	Black Powder	771	Match C	9	2	13	2488	8.0	11.0	98	2.6	2.4	0.89	3.0	0.98	79
19	Vert.	CBW	Black Powder	748	Match	12	8	21	2591	6.5	6.0	99	1.7	2.6	0.85	1.5	0.78	59

TABLE 3—*Continued.*

PB #	Align.	Material	Filler	Mass Fill (g)	Initiator	Number Frags Pipe Cap	Number Frags Total	Total Frag (g)	Avg Depth # tiles pipe cap		% Recovery	frag L/w	FWDM Slope	R^2	FWDMSA Slope	R^2	% Thin
71	Vert.	CBW	Black Powder	708	Hobby	17	13	31	2552	8.7	8.5	97	2.3	4	0.9	3.7	0.90	60
42	Vert.	CBW	Black Powder	735	DET	7	8	15	2551	6.5	3.3	98	1.3	0.5	0.91	0.1	0.53	79
85	FV	CBW	Black Powder	781	Match	0	5	5	677			26		0.2	0.86	0.2	0.86	
87	FV	CBW	Black Powder	764	Match	1	4	5	912			35		0.7	0.91	0.7	0.91	95
110	Hor.	CBW – US	Black Powder	746	Match	5	2	7	2084			76	2.3	0.7	0.96			61
Avg Black Powder @ match- frag wt 128g						**11**	**7**	**18**		**7.1**	**8.0**	**97**	**2.1**	**2.2**		**1.8**		
32	Vert.	CBW	TNT	635	DET	396	180	576	2075	11.2	9.6	82	3.3	72	0.95	56	0.98	51
81	FV	CBW	TNT	603	DET	75	21	96	394			15		7.6	0.93	7.6	0.94	61
80	FV	CBW	TNT	596	DET	46	14	60	399			15		2.7	0.95	2.7	0.95	61
83	FV	CBW	TNT+8g Pentolite	639	DET	57	25	82	765			19		3.1	0.77	3.1	0.77	59
88	Hor.	CBW – US	TNT flake	604	DET	82	30	112	1069			39	3.3	4.9	0.80			
66	Vert.	CBW	2400	621	DET	378	226	606	2198	11.6	10.7	84	3.6	49	0.91	41	0.97	51
67	Vert.	CBW	Red Dot	363	DET	211	141	>353	2255	11.3	11.2	86	7.3	26	0.93	15	0.99	38
31	Vert.	CBW	C4 (6″ long)	137	DET	230	140	>747	354	11.5	10.5	51	5.1	71	0.93	28	0.95	

as large or larger (*y*-axis) by the total recovered fragment weight allows the map to be used in the comparison of pipe bombs with unequal weight and size. FWDMs were plotted for all the pipe bombs used in test series A. The negative slope of the linear regression for each FWDM data set is listed in Tables 2 and 3. A steep slope is indicative of a powerful pipe bomb configuration. An exemplary FWDM is shown in Fig. 8 below.

Weighing each recovered pipe fragment could be difficult after an actual bombing incident. Another more simplified approach to fragmentation pattern analysis was devised which was complimentary to the use of FWDMs. Similar maps were constructed based on calculations including the surface area of the fragments as roughly measured with a handheld ruler. The slopes obtained from the linear regression of the surface area data treatment are also included in Tables 2 and 3, labeled "FSADM slope" (fragment surface area distribution mapping). The magnitudes of the FSADM slopes are comparable to those of the FWDM slopes. Neither the FWDM nor the FSADM slopes are absolute characterizations of pipe fragmentation. The numeric value of the slope can vary from shot to shot of identically configured pipe bombs. However, the relative magnitudes of the slopes are consistent and indicative of the type of explosive event. Figures 9 and 10 are plots of the FWDM or FSADM slope for each pipe on the *x*-axis versus the pipe diameter (12″ or 6″) and the initiation device [M (match) or D (detonator)] on the *y*-axis. The maps contain a purple line which is an experimentally determined slope threshold where any value to the right

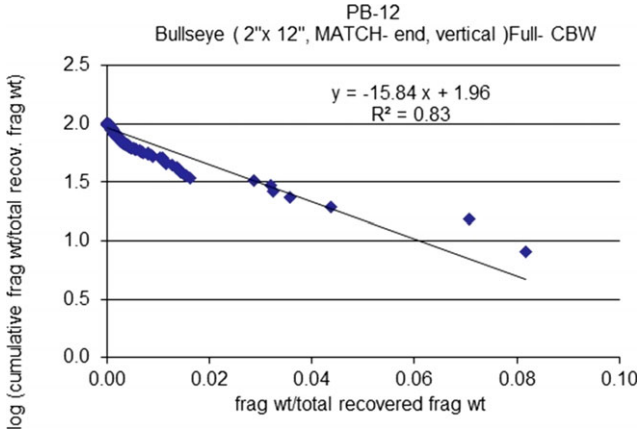

FIG. 8—*FWDM for 2″ × 12″ CBW steel pipe filled w/Bullseye initiated by match.*

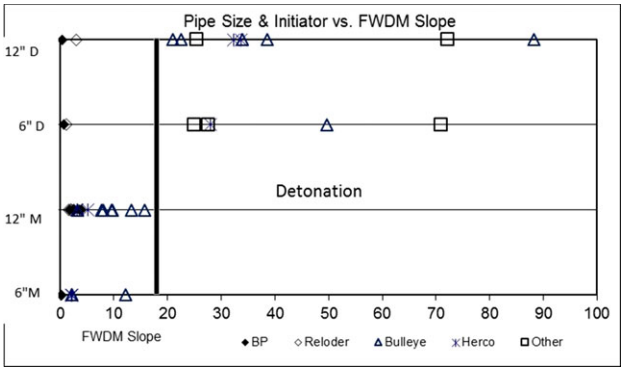

FIG. 9—*Pipe configuration versus FWDM slope.*

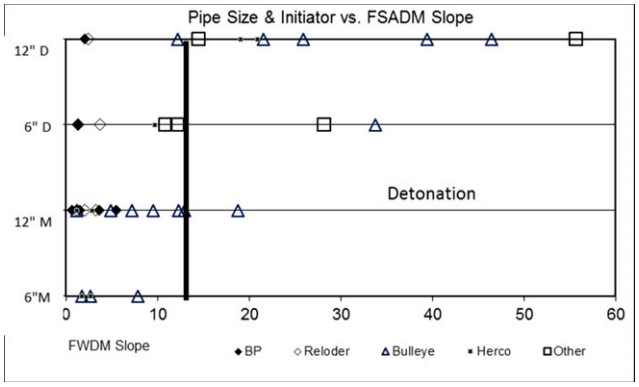

FIG. 10—*Pipe configuration versus FSADM slope.*

of the line indicates the corresponding pipe underwent a detonation, while any value to the left of the line indicates a deflagration. Nondetonations have low slope values and detonations have high slope values (Other factors considered in this evaluation are discussed below).

Observations used to evaluate "detonation" versus "deflagration" are listed below, and many of them are summarized in Table 3 for 2-inch by 12-inch steel pipes and Table 2 for 1-inch by 6-inch steel pipes and for PVC:

1 Average number of fragments
2 Average mass of fragments or mass of those greater than specified mass (i.e., 10 g)
3 Average length/mass ratio of recovered fragments
4 Average percentage thinning of fragments
5 Average depth fragment travelled into the recovery pack (test series A only)
6 Average overpressure at some specified distance from bomb (e.g., 20 ft, test series C only)
7 Average distance fragment travelled (test series D only)

Table 3, which compiles data for all the 2″ × 12″ pipe bombs, allows some interesting comparisons among fillers and among initiators. Among the Bullseye shots, the difference between the reaction initiated by a match versus a detonator manifests itself with half the number of fragments (339 vs. 608) which average twice the weight (6.7 vs. 3.4 g) of those created by the detonator. This difference is also seen in the values of FWDM and FWDMSA, but it is not observed in the depth of penetration into the tiles of the recovery test fixture. This latter observation foreshadows results in the free-field testing (Series D).

Velocity of Detonation (VOD) or Deflagration (Series A)

At the inception of this study, it was hoped that the rate of the burn or detonation could be used to characterize response as "deflagration" or "detonation." In practice, VOD data were difficult to obtain. Table 4 lists pipe bombs for which we attempted but failed to collect VOD data because the pipe did not detonate or other technical difficulties. Table 5 includes detonation velocity values for pipe bomb where rates were recorded at more than one location along the pipe. No clear differentiation among velocities from pipes containing different fillers was observed; values for which standard deviation could be established was within one standard deviation. Where no standard deviation is indicated in Table 5, data were available from only one make

TABLE 4—*Pipes for which VOD was attempted but failed.*

	2″ × 12″		
	Match	Detonator	1″×6″ det
RL-22	59	41,78,79	
IMR 4227		65,76,77	
Black powder	17,19,85,87		T1, 57
Bullseye	10, 53, 55, 63		73

wire. As a result, other postblast characteristics were used to evaluate whether the pipe bomb deflagrated or detonated.

Fragment Velocity (Series B)

Comparison between the flash panel data and high-speed camera data shows that the flash panels accurately recorded the time of fragment arrival. The fastest fragments consistently made electrical contact between the front and rear surfaces of the panels and caused a prominent flash that was observed by high-speed cameras. Slower fragments did not visibly flash and sometimes did not make contact between the front and rear surfaces. Pipes were oriented such that flash panels 2 and 4 recorded the arrival of pipe wall fragments, while flash panel 1 recorded the arrival of the initiating end cap and flash panel 3 recorded the arrival of the terminal end cap. Figure 11 includes all the fragments recorded from panels 2 and 4 (pipe wall fragments) for the three tests of pipe bombs filled with flaked TNT. The overall flash panel data showed groupings of faster fragments arriving first and centered around 1150 m/s, followed by a group of slower fragments in the range of 650 m/s. Velocity data from the end-cap fragments, panels 1 and 3, also showed a grouping of faster fragments followed by a grouping of slower fragments.

All the pipe bombs with measured fragment velocities showed a two-peaked velocity profile. In the more powerful fillers (Bullseye, IMR-4227, and TNT), the pipe wall fragments moved faster than the end-cap fragments, while in the slower burning fillers (Reloder 22 and black powder), the end-cap fragments travelled faster than the pipe wall fragments. Pipe bombs filled with more powerful fillers quickly overcame the strength of the pipe with very high internal pressures and threw the fragments radially out from the walls and axially from the end caps. The pressure relief from the fractured portions of the pipe was slow in comparison with the rate of detonation (VOD); thus, rupture of one portion of the pipe had little effect on other portions. Threaded portions of the end caps were also thrown radially, but they travelled slower because the threading is thicker and heavier than the pipe walls. This is probably the source of the slower group of fragments. Pipes filled with slower burning fillers experienced a slower and more uniform increase in internal pressure. The high-speed cameras showed that initial pipe rupturing occurred at the end cap with the initiator. Rupturing relieved pressure inside the pipe and had a strong effect on the fragmentation of the remaining pipe. One end of a fragment was free to be accelerated by the gases of combustion, while the other end was still attached to the body of the pipe. Kinetic energy was lost in pulling the pipe apart.

The fragments with the highest velocities are of primary importance because they represent the greatest damage potential and greater throw distances in an actual event. However, rather than characterizing the pipe bomb by a single fast-moving fragment, we have characterized the fragment velocity as the average of the "fast" grouping of fragments (Table 6).

TABLE 5—*Velocity of Detonation (VOD) measurements.*

Serial No.	Pipe Type	Pipe Size (in)	Filler	Filler Density (g/cm^3)	Initiator	Pipe Orientation	Average VOD (mm/μs)	VOD Std. Dev. (±mm/μs)
T-1	CBW	1 × 6	Flake TNT	0.87	Det	Horizontal	*N/A*	
PB-57	CBW	1 × 6	Flake TNT	0.86	Det	Vertical	*N/A*	
PB-83	CBW	2 × 12	Flake TNT	0.9	Det +8 g Pentolite	Horizontal	4.27	2.85
PB-32	CBW	2 × 12	Flake TNT	0.87	Detonator	Vertical	4.41	0.63
PB-33	PVC	2 × 12	Flake TNT	0.89	Detonator	Vertical	4.54	0
PB-60	PVC	1 × 6	Bullseye	0.71	Detonator	Vertical	3.77	0.31
PB-72	CBW	1 × 6	Bullseye	0.69	Detonator	Horizontal	4.6	0.93
PB-73	CBW	1 × 6	Bullseye	0.7	Detonator	Horizontal	N/A	
PB-10	CBW	2 × 12	Bullseye	0.67	Detonator	Vertical	N/A	
PB-53	CBW	2 × 12	Bullseye	0.7	Detonator	Horizontal (75% Full)	N/A	
PB-55	CBW	2 × 12	Bullseye	0.69	Detonator	Horizontal	N/A	
PB-37	CBW	2 × 12	Bullseye		Detonator	Vertical	4.33	0.27
PB-63	CBW	2 × 12	Bullseye	0.7	Detonator	Horizontal (50% Full)	N/A	
PB-64	CBW	2 × 12	Bullseye	0.69	Detonator	Horizontal	4.15	
PB-68	ERW	2 × 12	Bullseye	0.68	Detonator	Vertical	4.42	1.44
PB-69	CBW	2 × 12	Bullseye	0.66	Detonator	Horizontal	4.64	0.91
PB-74	CBW	2 × 12	Bullseye	0.68	Detonator	Horizontal	4.77	1.28
PB-75	CBW	2 × 12	Bullseye	0.7	Detonator	Horizontal	4.23	1.43
PB-67	CBW	2 × 12	Red Dot	0.52	Detonator	Vertical	3.91	
PB-41-2	CBW	2 × 12	Herco	0.61	Detonator	Vertical	4.46	0.89
PB-66	CBW	2 × 12	2400	0.89	Detonator	Vertical	3.93	

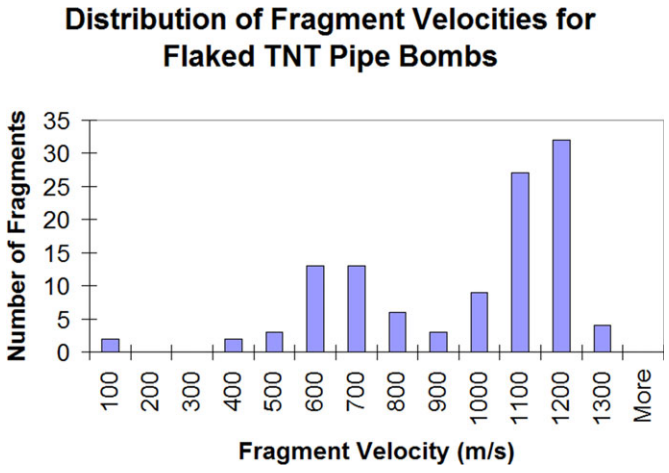

FIG. 11—*Histogram of pipe fragment velocities from 3 pipe bombs containing flaked TNT.*

TABLE 6—*Fragment velocity; average of the fastest group of fragments.*

PB	Energetic Filler	Initiator	Nominal size	Fragment Velocity (m/s) Pipe wall	Opposite end cap	Initiator end cap
72	Bullseye	DET	1″ × 6″	846	757	577
73	Bullseye	DET	1″ × 6″	811	845	597
74	Bullseye	DET	2″ × 12″	1081	850	518
75	Bullseye	DET	2″ × 12″	1078	864	579
76	IMR 4227	DET	2″ × 12″	1047	833	350
77	IMR 4227	DET	2″ × 12″	1048	824	321
80	TNT (flake)	DET	2″ × 12″	1099	917	297
81	TNT (flake)	DET	2″ × 12″	1086	856	311
83	TNT (flake)	DET*	2″ × 12″	1094	817	644
78	Reloder 22	DET	2″ × 12″	239	300	231
79	Reloder 22	DET	2″ × 12″	242	295	327
87	Black Powder	Match	2″ × 12″	242	143	355
85	Black Powder	Match	2″ × 12″	None	168	299

All pipes were CBW steel, 100% full, end initiated, shot horizontal seam down. Pipe wall was 274 cm and cap 258 cm from flash panel.
*Pentolite (8 g) was wrapped around detonator to increase output.

Blast Overpressure (Series C)

Table 7 includes pressure (psi) and impulse (psi-ms) measurements corrected to atmospheric pressure at sea level and a standard temperature of 59°F (15°C) for each of 26 pipe bombs. No appreciable variation of pressure was noted along the four different directions recorded; accordingly, results shown are averages of the four pressure values at the given distances. For pipe bombs placed above ground, ground reflections were present that would have affected the impulse measurements at the 15 and 20 foot gauges. Therefore, estimated TNT equivalences are based upon impulse measurements scaled to 10 feet. Figure 12 is an exemplary plot of incident overpressure versus scaled distance for the TNT charge (4). A least-squares third-order polynomial fit in log space for the measured data and that tabulated by Kingery-Bulmash (5,6) for a spherical charge in air has been applied to the data. The data at 10 foot scaled distance yielded a TNT equivalence of 48% for flaked TNT. This low yield was observed for all the flaked TNT charges, probably because the bulk density of flaked TNT (0.86 g/cm^3) was considerably lower than that of cast TNT (1.63 g/cm^3). This lower density was the reason the 1 inch diameter flaked TNT reference failed to detonate (5,6). Comparatively, cast TNT with density, 1.615 g/cm^3, has a reported critical diameter of 14.6 ± 2.0 mm (0.575 in) (7).

Plots such as Figure 12 were constructed for all the pipe bombs tested in series C. Given the small equivalence of the reference flake TNT charges and the Kingery-Bulmash tables (5), TNT equivalences of the pipe bombs were referenced directly to the Kingery-Bulmash tables and not to the flake TNT charges. The far right columns of Table 7 provide an estimate of these values; they were generally between 50 and 70% of cast TNT (slightly more powerful than flaked TNT).

Fragment Throw Distance (Series D)

There were two goals in this portion of the pipe bomb study. One was to determine how the various characteristics exhibited

TABLE 7—*Overpressure & impulse of pipe bombs at four distances and calculated TNT equivalence.*

Series	Initiator	Pipe Material	Filler	Fill wt. (g)	Height (in)	Pipe Orient	Pressure (psi)				Average Impulse Impulse (psi-ms)				TNT's TNT's TNTeq	TNT equivalence	
							5 ft	10 ft	15 ft	20 ft	5 ft	10 ft	15 ft	20 ft		Press	Impulse
Ref. (1)	Det	Cardboard	TNT flake	627	52	Hor	13	3.8	2.8	2.2	5.6	3.41	2.9	2.6	40%		
Ref. (9)	Det	Cardboard	TNT flake	323	52	Hor	5.2	1.91	1.3	1.0	2.3	1.11	0.8	0.9			
Ref. (4)	Det	Cardboard	TNT flake	643	52	Vert	21	4.89	2.6	2	6.7	3.06	2.8	2.6	48%		
Ref. (2)	Det	Cardboard	TNT flake	644	Ground	Hor	18	5.04	3.2	2.5	7.5	4.17	3.3	3	37%		
Ref. (3)	Det	Cardboard	TNT flake	637	Ground	Vert	14	4.94	2.9	2.3	6.4	3.93	2.8	2.5	36%		
Ref. (10)	Det	Cardboard	TNT flake	302	Ground	Hor	7.8	2.58	1.7	1.3	3.7	1.91	1.4	1.30			
PB-88	Det	CBW	TNT flake	604 AVE	Ground	Hor	18	5.82	3	2.1	7.8	4.98	3.7	2.9	40%		
PB-93	Det	PVC	Bullseye	456	52	Hor	23	6	3.8	2.7	8.4	4.28	3.4	3		0.69	0.64
PB-92	Det	CBW	Bullseye	480	52	Hor	18	5.44	3.2	2.3	6.7	4.13	3.7	3.2		0.59	0.59
PB-89	Det	CBW	Bullseye	481	Ground	Hor	21	6.16	3.4	2.5	8.3	5.41	4	3.2		0.67	0.77
PB-95	Det	CBW	Bullseye	479	Ground	Hor	22	6.09	3.6	2.8	9.3	4.87	3.7	3.3		0.67	0.70
PB-91	Match	CBW	Bullseye	487	52	Hor	15	4.25	2.7	2.1	5.5	3.34	2.5	2.5		0.46	0.47
PB-94	Match	CBW	Bullseye	477	Ground	Hor	22	5.64	3.8	2.7	8.3	4.13	3.4	3		0.62	0.59
PB-90	Match	CBW	Bullseye	492	Ground	Hor	19	6.57	3.5	2.5	7.9	5.34	3.8	3		0.70	0.74
PB-96	Match	CBW-50%	Bullseye	241	Ground	Hor	9.9	3.35	2	1.6	5.1	2.76	1.9	1.7		0.73	0.79
PB-98	Det	CBW	IMR-4227	652	Ground	Hor	15	4.96	2.9	2.2	6.9	4.51	3.3	2.6		0.40	0.47
PB-99	Match	CBW	IMR-4227	645	Ground	Hor	4.4	1.8	1	0.7	2.1	1.21	0.9	0.7		0.15	0.13
PB-97	Match	CBW	IMR-4227	667	Ground	Hor	5.8	2.01	1.3	1	2.8	1.54	1	0.9		0.16	0.16
PB-106	Match	CBW	Black powder	736	Ground	Hor	8.5	3.27	2.1	1.6	4.7	2.91	1.9	1.7		0.23	0.27
PB-110	Match	CBW	Black powder	746	Ground	Hor	9.7	3.54	2	1.6	5.4	3.48	2.5	2		0.25	0.32
PB-105	Match	PVC	Black powder	705	Ground	Hor	4.6	1.89	1.3	0.9	1.9	1.13	0.7	0.7		0.14	0.11
PB-107	Det	CBW	Reloder 22	703	Ground	Hor	5.9	2.53	1.5	1.1	3.1	1.87	1.3	1.1		0.19	0.18
PB-100	Match	CBW	Reloder 22	704	Ground	Hor	5.2	1.98	1.4	1	3.5	1.24	1	0.8		0.15	0.12
PB-108	Match	CBW	Reloder 22	753	Ground	Hor	5.2	2.27	1.3	1.0	2.7	1.62	1.1	0.9		0.16	0.15
PB-109	Match	ERW	Reloder 22	708	Ground	Hor	4	1.6	0.9	0.6	1.7	1.01	0.7	0.6		0.12	0.10
PB-101	Match	CBW-50%	Reloder 22	367	Ground	Hor	10	3.7	2.5	1.9	4.6	2.53	1.9	1.7		0.53	0.47

Steel pipes were either welded CBW or ERW.

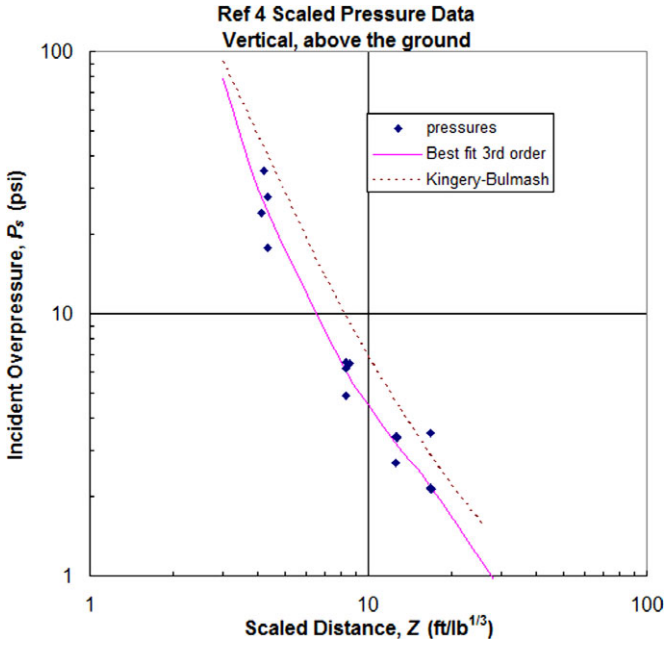

FIG. 12—*Scaled distance pressure curves for Ref. (4) plotted alongside Kingery-Bulmash data 5.*

by pipe bombs in the fragment recovery fixture compared to those of pipe bombs fired in an open field. Second was to determine the average and maximum distances the pipe bomb fragments would travel and to compare these distances to those predicted using simple literature models available.

When the pipe bomb fragments were unconfined, recovery dropped from an average of 87% to approximately 30%. The major test of the FWDM correlation was whether with such low recovery, a detonation could be recognized. Table 8 lists the pipe bombs tested for throw distance and their characterizing features in a side-by-side comparison with the data observed for these same pipe bomb configurations tested in the fragment recovery fixture. Interestingly, as the percentage of recovery decreases, the FWDM slope also decreases, probably because the missing fragments are the smaller fragments and these small fragments are responsible for steepening the slope. Nevertheless, detonations exhibited FWDM slopes greater than 13, and deflagrations had slopes less than 2. A 2″ diameter steel pipe filled with Bullseye smokeless powder and initiated with a match was still borderline with a slope of 8. Thus, as predicted (2), the FWDM slope correctly characterized the event with less than half of the pipe bomb fragments recovered.

There was not a clear difference in fragment throw distances between the high-power and low-power fillers. PB-89 filled with Bullseye and initiated with a detonator showed one of the shortest average fragment throw distances, only 79 m. A pipe bomb detonated with a comparable powder, IMR 4227, exhibited an average throw distance of 92 m. The data collected lend to the conclusion that regardless of the energetic filler, pipe bomb fragments from a bomb with roughly 500 to 700 g of filler can be expected to fly 100 m on average and can fly as far as 350 m. The average throw distances experimentally observed are in good agreement with the rule-of-thumb calculations for stand-off distances shown below with results in Table 9 (8,9). The equations used in references 8 and 9 are as follows:

TABLE 8—*Characterization of free-field pipe bombs compared to average of pipe bombs in test fixture; 2″ × 12″ steel pipe bombs, end initiated.*

				Individual results for pipes initiated in free field									Average fragment recovery for this filler in test fixture							
PB #	Pipe	Filler	Initiator	Filler wt (g)	% Recovery	FWDM slope	Ave. frag. L/D	Wt of ave frag (g)	Ave throw (m)	Max throw (m)	Wt (g) frag max distance	% Thinning	# Pipes ave	# Total Frags	% Recovery	FWDM slope	FWDMSA slope	Ave. frag. L/D	Wt of ave frag (g)	Tile depth	% Thinning
88	CBW – US	TNT flake	DET	604	39	13	3.3	9.5	99	329	19	66%	1	396	72	72	56	3.3	3.6	11.2	51
89	CBW – US	Bullseye	DET	481	23	24	3.0	4.2	79	252	1.0	51%	5	331	82	55	21	4.6	3.4	11.5	50
90	CBW – US	Bullseye	match	492	24	8.2	3.0	8.8	87	228	1.7	55%	8	385	84	14	7	2.9	6.7	11.5	50
98	CBW – US	IMR 4227	DET	652	43	23	3.3	8.5	92	343	17	65%	1	499	88	29	26	3.1	21	10.6	54
99	CBW – US	IMR 4227	match	645	60	0.8	2.2	37	75	234	3.5	87%	0	–	–	–	–	–	–	–	–
107	CBW – US	Reloder 22	DET	703	41	1.9	2.8	37	83	261	160	81%	1	55	99	3.0	2.4	3.4	48	7.1	72
108	CBW – US	Reloder 22	match	753	55	0.8	2.2	125	84	197	5.5	76%	2	12	98	2.2	1.4	2.8	203	8.1	64
109	ERW – Chinese	Reloder 22	match	708	34	0.7	2.2	79	77	224	468	83%	^	^	^	^	^	^	^	^	^
110	CBW – US	Black Powder	match	746	76	0.7	2.3	298	96	115	9.4	72%	5	18	97	2.2	1.8	2.1	128	7.1	87
	CBW	Herco	match										2	244	94	4.1	2.0	3.0	10	11.5	–
	CBW	Herco	DET										2	441	89	33	20	5.5	8	10.2	59
67	CBW	Red Dot	DET										1	380	86	26	15	7.3	6	11.3	38
66	CBW	2400	DET										1	606	84	49	41	3.6	4	11.6	51

D (safe distance in feet) = 600 × (explosive weight in pounds)$^{1/3}$ Ref. (8)
R (safe distance in meters for personnel) = 120 × (explosive weight in kilograms)$^{1/3}$ Ref. (9)

More sophisticated analysis of the throw distances has been offered in Ref. (10).

Figures 13, 14, and 15 illustrate various experimentally determined pipe fragment characteristics relative to performance as portrayed by the FWDM slopes. Figure 13 shows that the average percent of pipe wall thinning per pipe bomb levels off between 50 and 60% thinning at a FWDM slope of 10, a value associated with the threshold between deflagration and detonation.

TABLE 9—*Stand-off distances for devices calculated by two published models.*

TNT eq	Weight (g)	Kg eq TNT	Filler	Kinney & Graham (9)		Bomb Disposal Guide (8)	
				Meters	Feet	Feet	Meters
0.40	600	0.240	TNT (flaked)	75	245	485	148
0.67	490	0.328	Bullseye	83	272	539	164
0.16	650	0.104	IMR 4227	56	185	367	112
0.16	700	0.112	Reloder 22	58	190	377	115
0.25	750	0.188	Black Powder	69	225	447	136

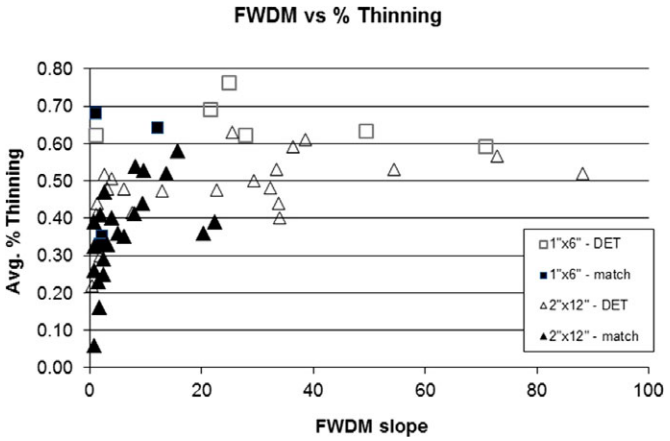

FIG. 13—*Average pipe wall thinning versus FWDM slope.*

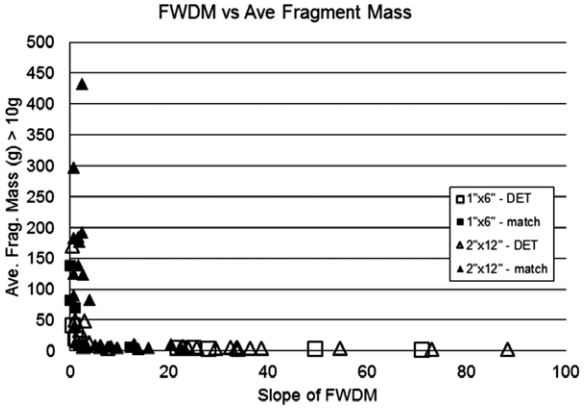

FIG. 14—*Average fragment mass (>10 g) versus FWDM Slope.*

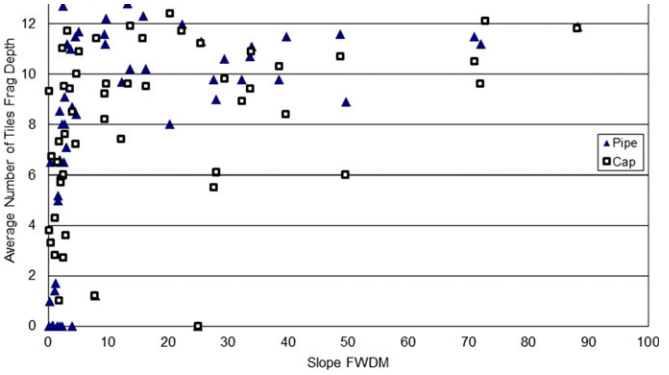

FIG. 15—*Average depth of penetration into recovery pack panels versus FWDM slope.*

Figure 14 plots the average recovered fragment mass of an individual pipe bomb for all fragments greater than 10 g. Clearly, the average mass dropped precipitously as the violence of the event (FWDM slope > 12) increased. Cursory analysis of the average mass of the fragments recovered is immediately suggestive of the power of a device. The percent of large fragments decreased as the FWDM slope increased. If the slope of the FWDM was greater than 10, 10% or less of the fragments were greater than 10 grams.

Figure 15 shows the average depth of penetration of pipe and end-cap fragments into the panels of the recovery fixture versus the slope of the FWDM for each pipe bomb. It is noteworthy that some fragments from pipe bombs with low FWDM slope values, that is, less power, were able to penetrate as far as those from more energetic pipe bombs. However, as expected, average penetration depths of the pipes with higher FWDM slope values were consistently higher.

Conclusions

This study summarizes results of nearly 150 pipes bombs, made of both PVC and steel (CBW or ERW), with nine different black and smokeless powder fillers. A gradation of performance between low-power pipe bombs, with fillers such as black powder or Reloder 22, and high-power fillers was not evident. Powerful fillers, such as Red Dot, Herco, and Bullseye, produced larger numbers of pipe fragments, smaller-sized pieces, and generally exhibited larger percentages of wall thinning than the less powerful fillers. Table 8 outlines some of the features observed from pipe bomb fragments.

Reproducible Results

Although different setups were used to recover pipe bomb fragments in the present test series than 6 years ago in the preliminary Technical Support Working Group (TSWG) study, results achieved in terms of type and extent of fragmentation, and ranking of factors affecting performance were identical (2). Thus, fragmentation results for two pipe bombs constructed and fired in an identical manner were duplicated over months in the same test protocol and over years in very different test arenas. *The duplication of pipe bomb fragmentation patterns, regardless of the test arena, is an important scientific discovery.*

Filler & Initiator

When initiated with RP-81 detonators, a variety of smokeless powders, both double base (Bullseye, Herco, Red Dot, and 2400) and single base (IMR 4227), clearly detonated in the 2″ × 12″ steel pipes. Bullseye and Herco also detonated using detonator initiation in 1″ × 6″ CBW steel pipes, and Bullseye in 1″ × 6″ PVC pipes. The explosions were noticeably less violent when electric matches were used for initiation. Hobby fuses appeared to initiate the devices the same as electric matches. Reloder 22, a low-power, single-base smokeless powder, and black powder did not detonate under any conditions.

Pipe Material

Most pipes used in this study, over 66, were continuous butt-welded (CBW) U.S. steel pipes, while seven electrical resistance-welded (ERW) Chinese steel pipes and eight PVC pipes were used for bomb construction. The main difference between the CBW and ERW pipes was how the seam responded to the event. In low-power events in the CBW pipes, the seam split open with a flat 90° angle edge. The same event in ERW pipes did not split on the seam, but split around or across the seam. Low-order events in PVC pipes left large fragments of pipe. For Reloder 22 filler in a 2″ diameter PVC pipe in duplicate tests, the lower half of the pipe remained intact when the initiator was located in the upper half. Black powder caused significant discoloration of the white PVC to an orange-brown color. High-order events in PVC pipe gave a large amount of very small melted fragments, which suggests the pipe was partially consumed.

Orientation of the Pipe

Horizontally oriented shots were performed using Bullseye in 2″ × 12″ CBW pipe. Most were initiated using an electric match, and little differentiation was observed between full and partially full pipes. Three horizontal pipe bombs were exploded with a detonator, and results suggest that a half-full pipe loaded with Bullseye may undergo detonation. Horizontal pipe bombs were characterized by one or two large fragment strips that spanned the entire length of the pipe (i.e., containing both sets of thread). These fragments were formed at the location of the pipe nipple in contact with the patio bricks.

Location of the Initiator

For most tests, the initiator was placed in the pipe through a hole drilled in the center of the end cap. Four pipe bombs were initiated using an electric match inserted into the pipe through a hole drilled in the center body directly opposite the seam. Three of the four side (center)-initiated shots produced slightly less fragments than similarly filled pipes which were end initiated (Table 3). The fourth shot, a repeat of one of the first three pipes, formed more fragments than end-initiated pipes. In all four cases, the slope of the FWDM was nearly identical for the side- and the end-initiated pipes. Thus, there appears to be no significant difference between side- and end-initiated pipes. However, these comparisons were made using only match-initiated pipe bombs which are such low-order events that differences may not be observed among pipe fillers.

Gurney Energy

During World War II, physicist Ronald Gurney developed a mathematical model for predicting the velocity of fragments driven by high explosives in a variety of geometries (11). For a cylindrical bomb, the Gurney equation is as follows:

$$\sqrt{2E} = V\sqrt{M/C + 1/2} \tag{2}$$

where V is the fragment velocity, M is the mass of the cylinder, C is the mass of the explosive charge, and $\sqrt{2E}$ is the Gurney energy, a characteristic property of the explosive material. The Gurney energy represents the amount of energy, per unit mass, that is available for kinetic energy of fragments and products of the decomposition. Gurney formulas have been demonstrated to predict fragment velocities for confined high explosive charges, in a variety of sizes and geometries (12). However, smokeless and black powders are not high explosives. A significant portion of the powder may burn after pipe rupture or may remain unburned.

The initial TSWG pipe bomb study (2) began with the question of whether or not fillers used in making pipe bombs were capable of detonating. The initial conclusion was that under some conditions they were capable of detonating. In this pipe bomb study, one of the goals was to test the hypothesis that a pipe bomb detonation could be modeled as a cylindrical bomb

TABLE 10—*Calculated gurney energies.*

PB	Energetic Filler	Initiator	Nominal size	Filler mass (g)	Fill density (g/cc)	Pipe mass (g)	Wall Velocity (m/s)	Gurney	
								Mass/charge (M/C)	$\sqrt{2E}$ (km/s)
72	Bullseye	DET	1″ × 6″	64	0.69	338	846	5.28	2.03
73	Bullseye	DET	1″ × 6″	66	0.69	338	811	5.12	1.92
74	Bullseye	DET	2″ × 12″	481	0.68	1549	1081	3.22	2.09
75	Bullseye	DET	2″ × 12″	485	0.69	1549	1078	3.19	2.07
76	IMR 4227	DET	2″ × 12″	642	0.92	1549	1047	2.41	1.79
77	IMR 4227	DET	2″ × 12″	678	0.95	1549	1048	2.28	1.75
80	TNT (flake)	DET	2″ × 12″	596	0.86	1549	1099	2.60	1.93
81	TNT (flake)	DET	2″ × 12″	603	0.85	1582	1086	2.62	1.92
83	TNT (flake)	DET*	2″ × 12″	639	0.90	1562	1094	2.44	1.88
78	Reloder 22	DET	2″ × 12″	696	1.00	1549	239	2.23	0.39
79	Reloder 22	DET	2″ × 12″	687	0.97	1549	242	2.25	0.40
87	Black Powder	Match	2″ × 12″	764	1.08	1537	242	2.01	0.38
85	Black Powder	Match	2″ × 12″				None		

All pipes were CBW steel, 100% full, end initiated, shot horizontal seam down.
*Pentolite (8 g) was wrapped around detonator to increase output.

using the Gurney model. This would allow the Gurney energy to be a filler characteristic, and it could be used to predict fragment velocities.

Using the fragment velocities measured in test series B (Table 6), Gurney energies were calculated and are tabulated in Table 10. Only the weight of the pipe, not the end cap, was included when calculating the ratio M/C. Pipe bombs containing Bullseye, which were proven to detonate, were anticipated to fit best using the Gurney model. Both 1″ and 2″ diameter Bullseye pipes, with significantly different M/C ratios, showed calculated Gurney energy values within 5% of one another. In this case, the Gurney model predicted fragment velocities. For the slower burning fillers which do not detonate, such as Reloder 22 and black powder, the Gurney model may not be valid. In fact, our experimental Gurney energy value for black powder 0.38 is significantly less than one published value of 0.94 (12).

The Gurney energy calculated for flaked TNT-filled pipe bombs in Table 10 is lower than published values for cast TNT (1.63 g/cm^3) of 2.37 km/s (12). We speculate that the lower bulk density of the TNT used in this study (0.86 g/cm^3) slowed the velocity of detonation, which reduced the efficiency of converting the mechanical energy available from the detonation into fragment velocities. In an attempt to obtain Gurney energy and VOD data that more closely matched published results, PB-83 included a small amount of Pentolite booster around the detonator to increase the output. The flaked TNT used in the same pipe was also packed at a somewhat higher density. The Gurney energy for this test was actually a little lower than for the other TNT tests, and the VOD was unchanged. The velocity of the adjacent end-cap fragments did increase, as shown in Table 6. [Note all but one of the pipe bombs shown in Table 10 initiated by a detonator. Pipe bombs initiated by match may give very different results.]

Of the pipe bomb configurations that were tested, there were both detonations and deflagrations. Fast-burning smokeless powders, such as Bullseye, Herco, IMR 4227, and TNT, detonated when initiated with a detonator in a 2″ diameter steel pipe; Bullseye was of sufficient energy that it also detonated in 1″ diameter pipe. Low-power fillers such as Reloder 22 and black powder did not detonate regardless of whether a detonator or match was used for initiation. Pipe fragmentation patterns were reproducible and showed distinctive characteristics relative to the number of fragments, their weight distribution, and pipe wall thinning. Detonation velocities of the pipe bombs with detonable fillers as well as fragment velocities and blast overpressures of all exploding pipe bombs were measured. These data could roughly be divided into performance typical of either high-power or low-power filler. Fragment throw distances were on average within the range of safe cordon distances at about 100 m. It was determined that the Gurney model could be used for detonating pipe bombs.

References

1. Bureau of Alcohol, Tobacco and Firearms. 1997 arson and explosives incidents report. Washington, DC: Department of Treasury, 1997.
2. Oxley JC, Smith JL, Resende E, Rogers E, Strobel RA, Bender EC. Improvised explosive devices: pipe bombs. J Forensic Sci 2001;46 (3):87–110.
3. Gregory O, Oxley J, Smith J, Platek M, Ghonem H, Bernier E, et al. Microstructural characterization of pipe bomb fragments. Mater Charact 2010;61(3):347–54.
4. Cooper PW. Explosives engineering. New York, NY: VCH Publishers Inc, 1996.
5. Kingery CN, Bulmash G. Airblast parameters rom TNT spherical air burst and hemispherical surface burst. Aberdeen Proving Ground, MD: Ballistic Research Laboratories, April 1984; Technical Report ARBRL-TR-02555.
6. Swisdak MM Jr. Explosion effects and properties part 1 – explosion effects in air. Silver Spring, MD: White Oak Laboratory, October 1975; NSWC/WOL/TR 75-116.
7. Popolato A, Gibbs TL. LASL explosive property data. Berkeley, CA: University of California Press, 1980;180.
8. Lenz RR. Explosives and bomb disposal guide, 2nd edn. Springfield, IL: Charles C. Thomas Pub, 1970;241–2.
9. Kinney GF, Graham KJ. Explosive shocks in air, 2nd edn. New York, NY: Springer-Verlag, 1985;6.
10. Oxley JC, Smith JL, Bakhtiyarov SI, Baldovi PM. A complex variable method to predict a range of arbitrary shape ballistic projectiles. J Appl Nonlinear Dyn, 2017;(6)2.
11. Gurney RW. The initial velocities of fragments from bombs, shells, and grenades. Aberdeen Proving Ground, MD: Ballistic Research Laboratories, 1943; BRL-405.
12. Kennedy JE. The Gurney model for explosive output for driving metal. In: Walters B, Zukas J, editors. Explosives effects and applications. New York, NY: Springer, 1998;221–35.

Additional information and reprint requests:
Jimmie C. Oxley, Ph.D.
Chemistry Department
University of Rhode Island
140 Flagg Road
Kingston, RI 02881
E-mail: joxley@chm.uri.edu